Journal of Photoscience (2003), Vol. 10(1), pp. 97–104

Excitation Wavelength Dependence of Laser Ablation Mechanism of Urethane-Urea Copolymer Film Studied by Time-Resolved Absorbance Measurements

Takuji Tada[1], Tsuyoshi Asahi[1], Hiroshi Masuhara[1]*, Masaaki Tsuchimori[2] and Osamu Watanabe[2]
[1]Department of Applied Physics, Osaka University, Suita, Osaka 565-0871, Japan
[2]Toyota Central Research and Development Laboratories Inc., 41-1, Yokomichi, Nagakute, Aichi 480-1192, Japan

The excitation wavelength dependence of laser ablation dynamics of an azobenzene-containing urethane-urea copolymer film was investigated by measuring the laser fluence dependence of etch depth, transient absorbance change at each excitation wavelength, and transient absorption spectra. Moreover expansion/contraction dynamics was studied by applying nanosecond time-resolved interferometry. The threshold was determined at several excitation wavelengths from etch depth measurement, while time-integrated absorbance was obtained under excitation conditions. The photon energy required to remove the topmost of surface layer of the film did not depend on excitation wavelength, and the penetration depth of excitation pulse dominated the etch depth. When the excitation wavelength was longer than 500 nm, permanent swelling was clearly observed but not for shorter wavelength excitation. In the latter case, photoisomerization occurred during excitation and the following photoreduction may play an important role. On the basis of the observations made in this study, a photochemical and photothermal mechanisms can explain mostly the short and long wavelength excitation results, respectively.

key words: laser ablation, spectroscopy, interferometry, polymer, azobenzene, photoisomerization, photoreduction

PHOTOCHEMISTRY AND MORPHOLOGICAL CHANGES

Since the framework of UV-visible (VIS) absorption and luminescence spectroscopy was established at the beginning of the twentieth century, molecular photochemistry has received much attention. The advent of flash photolysis techniques opened new research fields on intermolecular and intramolecular interactions and dynamics in the excited states and transient species. Owning to the invention of the laser in 1960 and the development of laser technology, the time resolution of spectroscopy has been improved from ns to fs order. On the other hand with the development of optical microscopy and electron microscopy, space-resolution has been very much improved in the late stage of the twentieth century. Laser microchemistry as space- and time-resolved photochemistry was started by combining laser and optical microscope techniques [1]. Furthermore innovation of scanning tunneling and scanning near-field optical microscopes makes it possible to observe the single molecule or atom, which is closely related to future photochemictry.

Minute amount changes in morphology and surface topography are induced by intense pulsed laser irradiation of materials, which forms new research area on solid state photochemistry. To directly probe such morphological changes it is necessary to apply imaging techniques that have favorably both time and space resolution, indeed, ultrafast imaging based on pump-probe method is very useful and has been applied. Irradiating pump pulse induces structural change, reaction, melting, phase transition, decomposition, fragmentation, and so on, and the accompanying spatial distribution of morphological changes are imaged by probe pulse. By varying the delay time between pump and probe pulses, we can trace such changes as a function of delay time. Actually laser induced morphological change was directly observed by developing and utilizing time-resolved imaging technique i.e. interferometry, surface light scattering, and optical microscopy, and so on [2-7].

Intense pulsed laser irradiation of organic materials generates high density excited states and their successive relaxation via various photochemical and photothermal processes eventually leads to morphological change. Thus it is important and indispensable to investigate the time evolution of not only mesoscopic morphological change as mentioned above but also the microscopic change in molecular and electronic structures.

Laser ablation of polymer film is one of the interesting phenomena which induce morphological changes as a result of irradiation with intense pulsed laser [8,9]. This has unique photophysical and photochemical characteristics and many researches have conducted to reveal its mechanism [2-5,8-28]. Photophysical and photochemical processes involved may depend on excitation wavelength (λ_{ex}), for example, solid material ejected during laser ablation of poly(methyl methacrylate) (PMMA) film changes depending on λ_{ex}, which was observed by scanning electron microscopy (SEM). The product at 248 nm excitation had melted and coalesced into spheres, while in the case of 193 nm excitation the product and ejected material

*To whom correspondence should be addressed.
E-mail : masuhara@ap.eng.osaka-u.ac.jp
Received & Accepted; October 23, 2002

did not show any signs of being heated to its melting point [17]. In the case of polyimide film the ablation rate showed Arrhenius-type exponential dependence on laser fluence at 248, 308, and 351 nm excitation, suggesting a photothermal process [18]. On the other hand the etch rate at 193 nm irradiation was linear with the fluence, which was explained in terms of photochemical process [18]. Triazene copolyester film irradiated at 266 and 308 nm, which correspond to the same $\pi-\pi^*$ transition, showed photochemical nature due to photolability of triazene groups [19].

Laser induced morphological dynamics of several polymer films were studied by use of nanosecond interferometry. In the case of PMMA film doped with biphenyl as a sensitizer, transient expansion started within excitation laser pulse width and then fragmented debris were ejected explosively [2]. While below the ablation threshold, rapid expansion was also observed, but the film was slowly contracted to the completely original flat surface. The morphological dynamics was considered in view of temperature elevation owning to efficient photothermal conversion and glass-rubber transition of PMMA [3]. Surface displacement dynamics due to laser-induced decomposition of triazenopolymer [4] and nitrocellulose films [5] were also directly measured and considered. Moreover laser-induced morphological dynamics of polyimide film at 248 and 351 nm excitation was studied [20]. Photochemical and photothermal processes can mostly explain morphological dynamics by 248 and 351 nm excitation, respectively. Laser induced morphological change is surely dependent on the kind of polymer and λ_{ex}. This indicates that such a morphological change reflects the difference of relaxation processes of high density excited states. Thus it is important to elucidate the electronic and molecular processes prior to morphological change and to understand how excitation evolves to expansion and ablation.

Studies on laser ablation mechanism need precise measurements of responsible molecular electronic excited states and/or chemical transient species under the ablation conditions. It was pointed out that absorbance at λ_{ex} changes during excitation [19,21-27]. In order to illustrate such absorbance change at λ_{ex} multiphotonic absorption process and reabsorption of transient species were considered. Fukumura, Masuhara, and coworkers proposed cyclic multiphotonic absorption for doped polymer film where lowest excited states absorb excitation photon repeatedly during excitation pulse [24]. From experiments and numerical calculation they revealed that via cyclic multiphotonic absorption sample temperature rose and laser ablation was induced. Fujiwara *et al.* studied laser ablation of pyrene-doped PMMA film at 248 nm excitation and reported that absorbance at the λ_{ex} gradually increased during laser irradiation and elucidated this phenomenon in terms of transient species (i.e. S_1, T_1, and cation of pyrene) [22]. Wang et al. investigated laser ablation of benzil or pyrene doped PMMA film and they explained fluence dependence of etch depth by considering absorbance change owning to photolysis and generation of excited state of dopant [25]. Furthermore, in the case of neat polymer film some researchers reported absorbance change during excitation [23,26,27].

IMPORTANCE OF EXCITATION WAVELENGTH DEPENDENCE

Transient species generated within excitation pulse play an important role in ns laser ablation of polymer films as described above. Thus for revealing the mechanism of laser ablation of polymer films, it is essential to measure transient absorption spectra to assign chemical species, to interrogate the absorbance change at λ_{ex} during high intensity excitation, and to observe the successive morphological change by utilizing various time-resolved methods. Moreover it is considered that changing the λ_{ex} is effective to derive further information on mechanism as photophysical and photochemical processes should change depending on λ_{ex}. However until now most experiments examined only one or few λ_{ex} [17-20,23,28].

In this article we have chosen urethane-urea copolymer containing azo chromophore at the side chain. Laser-induced morphological change of such a functionalized polymer film has received much attention as possible device fabrication of materials for future optical devices [29-31], high density memory [32,33], and so on. It is widely known that irradiation of light to the azo chromophore induces photoisomerization and photoreduction, so that elucidation of laser ablation mechanism of this polymer film is interesting for photophysical and photochemical study. Due to the broad absorption spectra of azo chromophore and optical parametric oscillator (OPO), we can elucidate laser ablation mechanism by tuning the λ_{ex}.

At the longer wavelength excitation ($\lambda_{ex} \geq 500$ nm) permanent swelling was observed which was not clearly observed in the case of shorter wavelength excitation ($\lambda_{ex} < 500$ nm). Transient absorbance at the excitation wavelength and transient absorption spectra were measured, and laser induced expansion/contraction dynamics was measured by utilizing nanosecond interferometry. On the basis of these results, we discuss λ_{ex} dependence of laser ablation mechanism and the role of photoisomerization and photoreduction.

MATERIAL AND METHODS

Sample

Sample film was prepared by spin-coating 15 wt% pyridine solution of urethane-urea copolymer on a quartz plate. The film was baked for 20 hr at 100°C and successive 2 hr at 150°C in vacuum to remove the residual solvent. Film thickness was 1.7 μm. For transient absorbance and transient spectral measurement, films with thickness of 180 nm and 190 nm were prepared, respectively. Figure 1 shows its chemical structure and UV -VIS absorption spectrum. The broad absorption band in VIS region is ascribable to the trans isomer, since cis isomer is not stable at

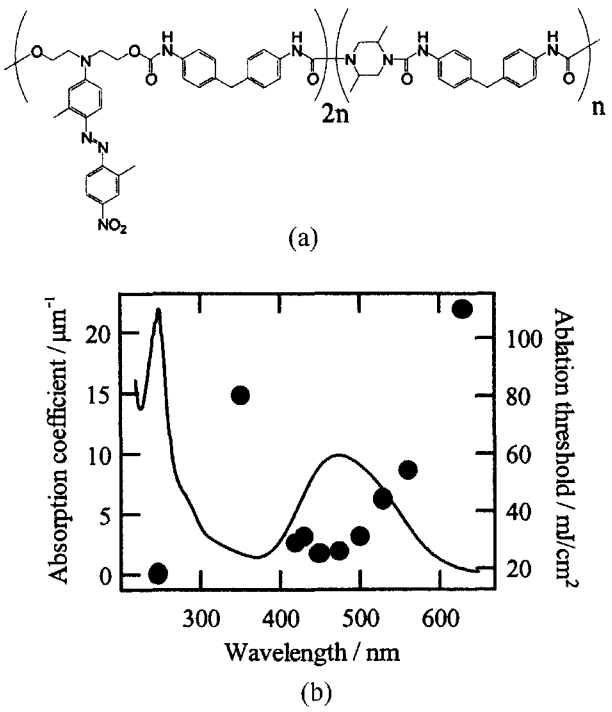

Figure 1. (a) Chemical structure of urethane-urea copolymer film. (b) Absorption spectra of the film and its threshold (●) as a function of excitation wavelength.

room temperature owing to the rapid thermal cis to trans isomerization [34].

Ablation experiment

A KrF excimer laser (Lambda Physik Lextra 200, 248 nm, 30 ns fwhm), XeF excimer laser (Lambda Physik Lextra 200, 351 nm, 30 ns fwhm), or tunable OPO (Continuum Surelite OPO) pumped by the 3rd harmonic pulse of a Q-switched Nd^{3+}: YAG laser (Continuum Surelite 2, 355 nm 10 ns fwhm) was used as an excitation pulse for inducing ablation. The fluence was adjusted by use of partially transmitting laser mirrors for excimer lasers and ND filter for OPO beam. A central area of the laser pattern was chosen with an appropriate aperture and then focused onto the sample surface by using a quartz lens (f = 200). Fresh surface of the sample film was chosen for all experiments. The depth profile was measured by a surface profiler (Sloan, Dektak 3), and the etch depth was obtained as a difference of averaged levels between non-irradiated area and irradiated one.

Transient absorbance measurement at the excitation wavelength

Transient absorbance of the film at λ_{ex} was measured by using two photodiodes [21,22]. A small part of the incoming laser pulse was separated by a quartz plate and detected by the first photodiode, while the transmitted laser pulse was simultaneously detected by the second photodiode. The signals from two photodiodes were recorded by a digital oscilloscope and then transient or time-integrated absorbance was calculated.

Transient absorption spectral measurement

In this experiment the 2nd harmonic pulse of a Q-switched Nd^{3+}: YAG laser (Continuum Surelite 1, 532 nm 10 ns fwhm) was used as an excitation pulse. The monochromatic pulse of OPO system or the 3rd harmonic pulse of Q-switched Nd^{3+}: YAG laser was divided into two by a quartz plate; one as a probe pulse and the other as a reference pulse. The probe pulse was introduced to the sample surface with a normal angle. Transmitted probe pulse and reference one were detected with two photodiodes and recorded by a digital oscilloscope. Transient absorption was calculated from these two signals. By varying the output wavelength of the OPO system, we could obtain absorption spectra. Time-resolved measurement was carried out by changing the delay time (Δt) between excitation light and probe light. The delay time was controlled by a digital delay/pulse generator (Stanford Research System, DG 535) and monitored shot by shot with a digital oscilloscope. Here we define $\Delta t = 0$ as the time when the both peaks of excitation and probe pulses were coincided with each other.

Nanosecond time-resolved interferometry

The system of nanosecond time-resolved interferometry applied here is same as reported before [2-5]. A XeF excimer laser was used as an excitation pulse and a probe pulse was the second harmonic pulse of a Q-switched Nd^{3+}: YAG laser. Time-resolved measurement was carried out by a similar manner as mentioned above, while nanosecond interference patterns were acquired by a CCD camera. In the experiment, a shift of one fringe spacing to the left or right corresponds to an expansion or etching of 266 nm, that is, a half wavelength of the probe laser. All measurements were carried out at room temperature in air. All data were obtained by one-shot measurements in order to avoid effects brought about by exciting photoproducts formed by previous irradiation.

RESULTS AND DISCUSSION

Excitation wavelength dependence of etch depth

Upon intense pulsed laser irradiation, the sample film undergoes permanent morphological changes. Figure 2(a) shows fluence dependence of etch depth obtained by changing the λ_{ex} from UV to VIS region. The negative value indicates the average level of irradiated area becomes higher than that of non-irradiated area due to surface elevation. In this paper we call this phenomenon as permanent swelling. In the case of $\lambda_{ex} < 500$ nm, the laser-induced permanent swelling was not clearly observed and the etch depth increases monotonously with the laser fluence. On the other hand, at longer λ_{ex} ($\lambda_{ex} \geq 500$ nm), the film first showed permanent swelling and underwent etching with further increase of the laser fluence. The maximum height of the permanent swelling was increased with λ_{ex}, and furthermore etch rate is larger as λ_{ex} increases. Figure 2(b) shows some optical microscopic images of irradiated area at 430 nm

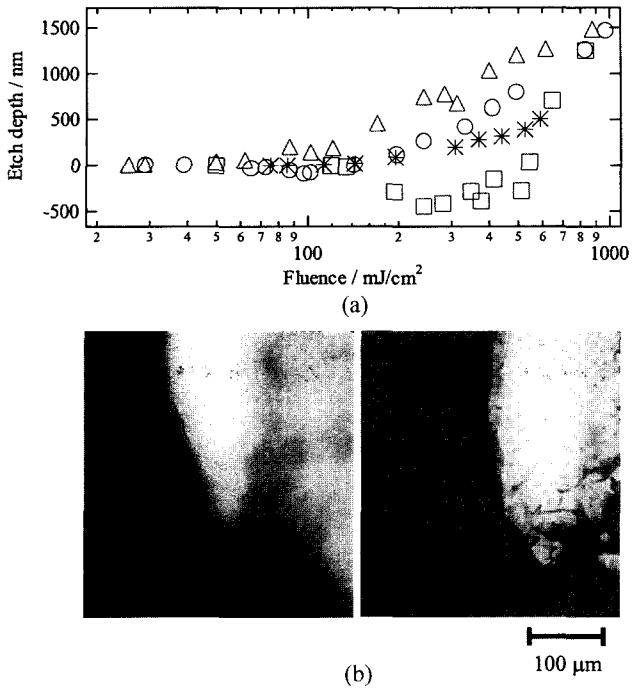

Figure 2. (a) Etch depth and expansion height as a function of laser fluence. Excitation wavelength is 351 nm (*), 475 nm (△), 530 nm (○), and 630 nm (□). (b) Optical microscopic images obtained for 430 nm excitation and 170 mJ/cm^2 (left side) and for 560 nm excitation and 250 mJ/cm^2 (right side). White and gray areas in the image correspond to ablated and non-ablated areas, respectively.

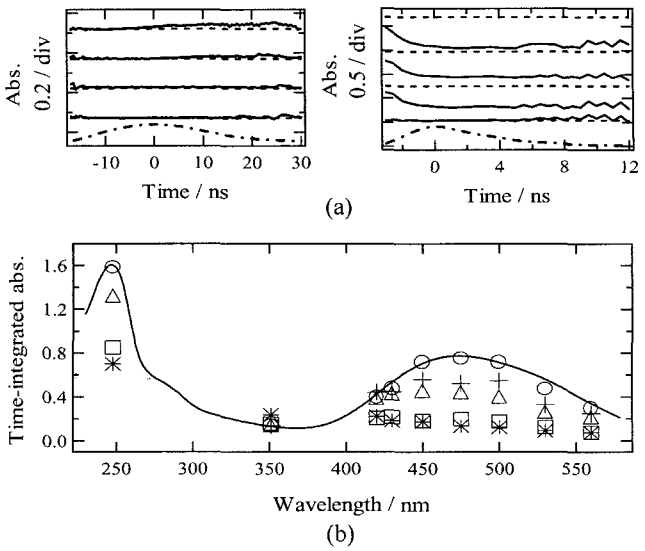

Figure 3. (a) Transient absorbance change at 351 nm (left side) and 475 nm excitation (right side). Fluence was 43, 64, 150, and 290 mJ/cm^2 at 351 nm excitation and 1, 26, 70, and 250 mJ/cm^2 at 475 nm excitation from bottom to top. Dotted lines and dash dotted one are absorbance at the excitation wavelength and the temporal profile of excitation pulse, respectively. (b) Time-integrated absorbance at each excitation wavelength, very low fluence (○), 10 mJ/cm^2 (+), near the threshold (△), 200~300 mJ/cm^2 (□), and effective absorbance (*). The solid line is absorbance of the ground state at each wavelength, representing conventional absorption spectrum.

excitation (left side) and 560 nm excitation (right side), respectively. The bad uniformity of etched area is due to poor pulse profile of OPO system. When the λ_{ex} is longer than 530 nm, fibrous residues were observed on the irradiated surface as shown in Figure 2(b). On the contrary such residues were not clearly observed at shorter λ_{ex}. The ablation or swelling threshold (minimum fluence where permanent morphological changes were observed) at each λ_{ex} was determined and plotted in Figure 1(b). Hereafter we simply call both values the threshold in this paper. It is general to consider that the etch rate depend on the penetration depth of excitation pulse and the threshold is related to absorption coefficient of polymer film. When absorption coefficient is small, the ablation threshold is high, and vice versa. Permanent morphological changes induced by intense laser irradiation clearly depended on λ_{ex}.

Transient absorbance change at the excitation wavelength

Figure 3(a) shows transient absorbance change at 351 nm and 475 nm excitation, respectively, where the film thickness was 180 nm. In the case of 351 nm absorbance change was too small to detect, so we use more thick film and correct the difference of film thickness. At the fluence far lower than the threshold the absorbance remained constant during excitation at each excitation wavelength and its value is quiet similar to that obtained by the conventional spectrometer. This indicates that absorbance change was too small to detect or any appreciable reaction was not induced. In the case of 351 nm excitation, the absorbance gradually increased during excitation at 100 mJ/cm^2. When we increased the fluence a similar but faster absorbance increase was observed. On the contrary, the absorbance decreased during excitation at 475 nm and with increase in the fluence the absorbance change gradually became large. The similar absorbance decrease was observed at $\lambda_{ex} \geq$ 430 nm, which was confirmed by systematic examination like Figure 3(a).

Time-integrated absorbance at each excitation wavelength was calculated for different fluence and plotted in Figure 3(b). At the fluence far lower than threshold, the time-integrated absorbance was similar to the conventional absorption spectrum of the film. At 248 nm and 430 nm~560 nm, time-integrated absorbance was decreased with increase in fluence, while at 351 nm time-integrated absorbance was increased a little with increase in laser fluence. In the case of 420 nm excitation, time-integrated absorbance did not change appreciably until about 20 mJ/cm^2 and then it decreased with further increase in fluence.

Transient absorption spectral measurement

Transient absorption spectra of urethane-urea copolymer film at several delay times are summarized in Figure 4. The λ_{ex}

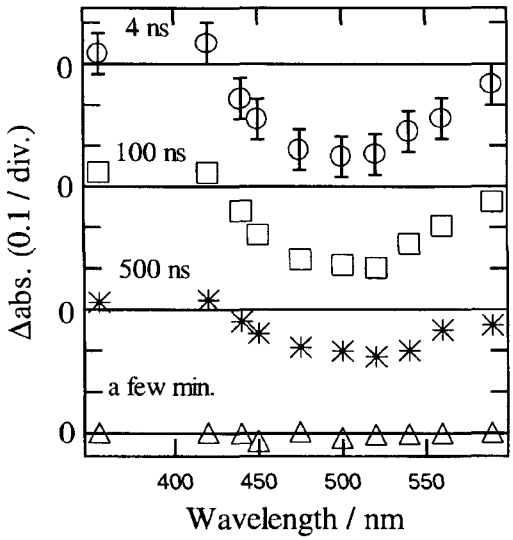

Figure 4. Transient absorption spectral obtained at the fluence of 35 mJ/cm^2 for 532 nm excitation. The delay time is given in the corresponding frame.

and fluence were 532 nm and 35 mJ/cm^2 below the threshold, respectively. At 4 ns a small absorbance increase was observed at 355 nm and 420 nm and bleaching was observed at wavelength longer than 430 nm. These absorbance changes (Δabs) gradually relaxed with time evolution and after a few min later original absorbance was recovered within the experimental error. It suggests that most of azo chromophore was not decomposed or was not lost even after the laser irradiation at this experimental condition.

As Δabs was -0.22 and -0.17 at 520 nm and 540 nm for 4 ns delay, respectively, it is presumed that Δabs at 530 nm was between -0.22 and -0.17. From the result of transient absorbance measurement, Δabs (at 530 nm excitation, 37 mJ/cm^2 and 4 ns delay) was -0.20 which coincides with that of transient absorption spectral measurement. Here we assumed that the difference of experimental conditions such as λ_{ex}, fluence, and film thickness were enough little to ignore.

Naito *et al.* reported UV-VIS absorption spectrum changes during photoisomerization of 4-dimethylamino-4'-nitroazobenzene (DANAB) in polyetherimide film [34]. The absorbance around 490 nm was decreased with the increase of concentration of cis isomer. On the contrary absorbance around 400 nm was increased. This result resembles to the present work and chemical structure of DANAB is very similar to azo chromophore of our sample. Thus we infer that the transient absorbance change shown in Figure 4 corresponds to the photoisomerization.

Expansion and contraction dynamics below the threshold

Surface morphological change at 351 nm excitation and a laser fluence of 70 mJ/cm^2, below the threshold, was measured. By analyzing the fringe patterns the surface displacement was estimated as a function of delay time and plotted in Figure 5.

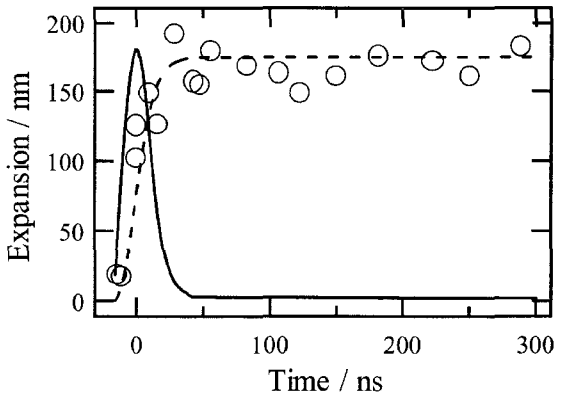

Figure 5. Expansion and contraction dynamics at 351 nm excitation, where the fluence was 70 mJ/cm^2 below the threshold. The solid and dashed curves represent the temporal profile of the excimer laser pulse and its time-integration, respectively.

The surface expands during excitation and reaches the maximum value at the end of the pulse and then the film undergoes μs-order contraction. After a few min later we could not observed any permanent fringe shifts, that is, the film completely contracted to original surface.

Relationship among absorbance at λ_{ex}, etch depth, and threshold

Absorbance, etch depth, and threshold, which are key parameters to understand laser ablation mechanism, correlate with each other. Thus on the basis of experimental results and some assumptions we discuss the relationship between these factors. According to Lambert's law the laser fluence after passing through the layer, I, is given by

$$I = I_0 \exp(-\alpha d) \quad (1)$$

Here I_0, d, and α are the incident laser fluence, thickness of the layer, and absorption coefficient, respectively. If we assume that Lambert's law holds under our experimental conditions and etching proceeds until the depth where intensity of the excitation pulse reduces to the etching threshold, the etch depth, d, is represented by the following simple equation [19]:

$$d = \alpha_{eff}^{-1} \ln(I_0/I_{th}) \quad (2)$$

Here α_{eff} is defined as effective absorption coefficient when ablation was induced, and I_{th} is the etching threshold. By comparing Eq. (2) with the result of etch depth measurements in Figure 2(a) it is clear that α_{eff}^{-1} is not constant, which may correspond to increasing rates of etch depth for the fluence. α_{eff} is estimated from the result of etch depth measurement for all λ_{ex} and plotted in Figure 3(b) with asterisk marker (*) after converted into absorbance. It is worth noting that converted α_{eff} into absorbance is not consistent with the conventional absorption spectrum but quite close to time-integrated absorbance under intense excitation condition at all λ_{ex}. Thus our results are mostly explained by considering that penetration depth of

excitation pulse dominates etch depth.

Absorbance change was also induced during excitation near the threshold as shown in Figure 3(a). Thus, by using Eq. (1) and time-integrated absorbance near the threshold (α_{th}), we estimated the absorbed energy by the film whose thickness is 180 nm. It was about 17 mJ/cm^2 at all λ_{ex}. It is interesting feature that the energy to induce permanent morphological changes of the film surface is not depending on the λ_{ex}.

Laser ablation mechanism

Fujiwara *et al.* previously reported laser ablation dynamics of PMMA film doped with 5-diazo Meldrum's acid (DM) [21]. The topmost surface layer absorbed enough energy and left the film, while the deeper part not absorbing enough energy expanded to form a new surface which is higher than the original one. They considered that the permanent swelling is due to incomplete fragmentation and displacement of the deeper part of the film. Furthermore they calculated the amount of photodecomposed DM, which corresponds to amount of generated N_2, and showed that photodecomposition of the dopant is not a main factor of the permanent swelling. They concluded that photothermal processes are dominant for inducing the permanent swelling even for polymer film containing photodecomposable dopant.

Here we discuss the laser ablation mechanism of urethane-urea copolymer film in terms of penetration depth of the excitation pulse, photochemical, and photothermal processes. In the case of 248 nm, 430 nm, 450 nm, and 475 nm excitation, almost incident energy was absorbed at the topmost surface layer because of high α_{th}. On the other hand, at 351 nm, 420 nm, and 500 nm~560 nm excitation, incident energy was partly absorbed at the surface layer and residual energy was absorbed at the underlying layer. At 500 nm~560 nm excitation, α_{th} was decreased with increase in λ_{ex} and height of the permanent swelling showed opposite tendency. Thus it is considered that due to the increase in penetration depth of excitation pulse deeper part of the film contribute to the permanent swelling and height of the permanent swelling was increased. These results were consistent with the result reported by Fukumura *et al.* [11]. On the other hand, the permanent swelling was not clearly observed at 351 nm and 420 nm excitation, which means that excited deeper part of the film did not contribute to the permanent swelling. This result implies that energy dissipation mechanism should be different, maybe, photochemical processes play an important role in these wavelength regions.

Ronayette *et al.* studied the photoreduction of azobenzene in isopropanol and reported that only the cis isomer is photoreducible [36]. Watanabe *et al.* reported that irreversible photobleaching of polyurethane and urethane-urea copolymer film was caused by reduction [37]. It is widely known that reduction of azo dyes eventually produces a series of anilines [38-40]. Furthermore Vydra *et al.* reported that, from IR-spectroscopy and GPC measurements, excited azo dye causes not only a destruction of itself but also a partial degradation of the polymer backbone [41]. Thus if we assume that initial stage of photoreduction are common for our sample and azobenzene, photodegradation of our sample is induced via cis isomer. According to the result of our transient absorption spectral measurement and other researcher's previous report [42], it is considered that cis isomer of our sample possesses the broad absorption band around 400 nm and photodegradation is effectively induced by excitation at this band. Consequently, decrease of time-integrated absorbance at 420 nm excitation may be ascribed to photodegradation.

In the case of high fluence excitation, time-integrated absorbance at shorter λ_{ex} ($\lambda_{ex} < 530$ nm) was larger than that of longer one as show in Figure 3(b). In other words, penetration depth of excitation pulse at shorter λ_{ex} is shallower than that of longer one. When the excitation pulse of same intensity is introduced to the sample film, the thickness of excited surface layer is larger for shorter λ_{ex} than for longer one. That is, density of excited state becomes higher for shorter λ_{ex}. Moreover not only thermal degradation but also photochemical decomposition occur at the shorter λ_{ex} as considered above. Thus it is considered that irradiated polymer was more effectively decomposed into small fragments at shorter λ_{ex}. This is consistent with optical microscopic images shown in Figure 2(b).

CONCLUSION

Now we summarize possible laser ablation mechanism of urethane-urea copolymer film on the basis of the present results. Trans isomer is first excited and then some is partly converted into cis isomer owing to photoisomerization during excitation. In the case of shorter λ_{ex}, generated cis isomer reabsorbs the excitation photons and successive degradation of polymer maybe brought about. The sudden volume expansion owing to generation of small decomposed products and/or temperature elevation becomes large enough to induce volume explosion, leading to ablation. Moreover it is considered that transient expansion of the film surface below the ablation threshold shown in Figure (5) is caused owing to such a volume expansion. On the other hand, in the case of longer λ_{ex} in which cis isomer might have low molar absorptivity, reabsorption by cis isomer is little. Thus photon energy absorbed by trans isomer is eventually converted to heat via vibrational relaxation, resulting in rapid temperature elevation and as a result permanent swelling and ablation are induced.

Although our proposed mechanism seems to explain the experimental results presented here, still several questions are left. Why the energy required for inducing permanent morphological change does not depend on λ_{ex}, consequently, ablation mechanism? Which mechanism brings about transient expansion and contraction as shown in Figure (5); thermal expansion or volume expansion due to generation of small decomposed products via photochemical processes? Thus further experiment is indispensable to answer these questions and to confirm our mechanism. Time-resolved interferometric

measurement at several λ_{ex} is now in progress in our laboratory.

Mechanistic study on laser ablation is indeed one of representative research areas of solid state photochemistry. Combination of time-resolved spectroscopy with time-resolved imaging method is surely important and indispensable, which is opening new photochemical studies.

REFERENCES

1. Masuhara, H. (1994) *Microchemistry: Spectroscopy and Chemistry in Small Domains.* Ed. by H. Masuhara, F. C. DeSchryver, N. Kitamura and N. Tamai, North-Holland pp. 3-20.
2. Furutani, H., H. Fukumura and H. Masuhara (1994) Nanosecond time-resolved interferometric study on morphological dynamics of doped poly(methyl methacrylate) film upon laser ablation. *Appl. Phys. Lett.* **65**, 3413-3415.
3. Furutani, H., H. Fukumura and H. Masuhara (1996) Photothermal transient expansion and contraction dynamics of polymer films by nanosecond interferometry. *J. Phys. Chem.* **100**, 6871-6875.
4. Furutani, H., H. Fukumura, H. Masuhara, T. Lippert and A. Yabe (1997) Laser-induced decomposition and ablation dynamics studied by nanosecond interferometry. 1. A triazenopolymer film. *J. Phys. Chem. A* **101**, 5742-5747.
5. Furutani, H., H. Fukumura, H. Masuhara, S. Kambara, T. Kitaguchi, H. Tsukada and T. Ozawa (1998) Laser-induced decomposition and ablation dynamics studied by nanosecond interferometry. 2. A reactive nitrocellulose film. *J. Phys. Chem. B* **102**, 3395-3401.
6. Hatanaka, K., T. Itoh, T. Asahi, N. Ichinose, S. Kawanishi, T. Sasuga, H. Fukumura and H. Masuhara (1998) Time-resolved surface scattering imaging of organic liquids under femtosecond KrF laser pulse excitation. *Appl. Phys. Lett.* **73**, 3498-3500.
7. Hatanaka, K., Y. Tsuboi, H. Fukumura and H. Masuhara (2002) Nanosecond and femtosecond laser photochemistry and ablation dynamics of neat liquid benzenes. *J. Phys. Chem. B* **106**, 3049-3060.
8. Srinivasan, R. and V. M. Banton (1982) Self-developing photoetching of poly(ethylene terephthalate) films by far-ultraviolet excimer laser radiation. *Appl. Phys. Lett.* **41**, 567-578.
9. Kawamura, Y., K. Toyoda and S. Namba (1982) Effective deep ultraviolet photoetching of polymethyl methacrylate by an excimer laser. *Appl. Phys. Lett.* **40**, 374-375.
10. Masuhara, H., H. Hiraoka and K. Domen (1987) Dopant-induced ablation of poly(methyl methacrylate) by a 308-nm excimer laser. *Macromolecules* **20**, 450-452.
11. Fukumura, H., N. Mibuka, S. Eura and H. Masuhara (1991) Porphyrin-sensitized laser swelling and ablation of polymer films. *Appl. Phys. A* **53**, 255-259.
12. Chen, S., I.-Y. S. Lee, W. A. Tolbert, X. Wen and D. D. Dlott (1992) Application of ultrafast temperature jump spectroscopy to condensed phase molecular dynamics. *J. Phys. Chem.* **96**, 7178-7186.
13. Pettit, G. H. and R. Sauerbery (1993) Pulsed ultraviolet laser ablation. *Appl. Phys. A* **56**, 51-63.
14. Bennett, L. S., T. Lippert, H. Furutani, H. Fukumura and H. Masuhara (1996) Laser induced microexplosions of a photosensitive polymer. *Appl. Phys. A* **63**, 327-332.
15. Zhigilei L. V., P. B. S. Kodali and B. J. Garrison (1998) A microscopic view of laser ablation. *J. Phys. Chem. B* **102**, 2845-2853.
16. Arnold, N. and N. Bityurin (1999) Model for laser-induced thermal degradation and ablation of polymers. *Appl. Phys. A* **68**, 615-625.
17. Srinivasan, R., B. Braren, D. E. Seeger and R. W. Dreyfus (1986) Photochemical cleavage of a polymeric solid: details of the ultraviolet laser ablation of poly(methyl methacrylate) at 193 and 248 nm. *Macromolecules* **19**, 916-921.
18. Küper, S., J. Brannon and K. Brannon (1993) Threshold behavior in polyimide photoablation: single-shot rate measurements and surface-temperature modeling. *Appl. Phys. A* **56**, 43-50
19. Hahn, Ch., T. Lippert and A. Wokaun (1999) Comparison of the ablation behavior of polymer films in the IR and UV with nanosecond and picosecond pulses. *J. Phys. Chem. B* **103**, 1287-1294
20. Masubuchi, T., T. Tada, E. Nomura, K. Hatanaka, H. Fukumura and H. Masuhara (2002) Laser-induced decomposition and ablation dynamics studied by nanosecond interferometry. 4. A polyimide film. *J. Phys. Chem. A* **106**, 2180-2186.
21. Fujiwara, H., Y. Nakajima, H. Fukumura and H. Masuhara (1995) Laser ablation dynamics of a poly(methyl methacrylate) film doped with 5-diazo Meldrum's acid. *J. Phys. Chem.* **99**, 11481-11488.
22. Fujiwara, H., H. Fukumura and H. Masuhara (1995) Laser ablation of a pyrene-doped poly(methyl methacrylate) film: dynamics of pyrene transient species by spectroscopic measurements. *J. Phys. Chem.* **99**, 11844-11853.
23. Pettit, G. H., M. N. Ediger, D. W. Hahn, B. E. Brinson and R. Sauerbrey (1994) Transmission of polyimide during pulsed ultraviolet laser irradiation. *Appl. Phys. A* **58**, 573-579.
24. Fukumura, H. and H. Masuhara (1994) The mechanism of dopant-induced laser ablation. Possibility of cyclic multiphotonic absorption in excited states. *Chem. Phys. Lett.* **221**, 373-378.
25. Wang, J., H. Niino and A. Yabe (1999) Laser ablation of poly(methylmethacrylate) doped with aromatic compounds: laser intensity dependence of absorption coefficient. *Jpn. J. Appl. Phys.* **38**, 871-876.
26. Tsuboi, Y., S. Sakashita, K. Hatanaka, H. Fukumura and H. Masuhara (1996) Photothermal ablation of polystyrene film by 248 nm excimer laser irradiation: a mechanistic study by time-resolved measurements. *Laser Chem.* **16**, 167-177.
27. Masubuchi, T., H. Fukumura and H. Masuhara (2001) Laser-induced decomposition and ablation dynamics studied by nanosecond interferometry 3. A polyurethane film. *J. Photochem. Photobiol. A Chem.* **145**, 215-222.
28. Hauer, M., T. Dickinson, S. Langford, T. Lippert and A. Wokaun (2002) Influence of the irradiation wavelength on the ablation process of designed polymers. *Appl. Surf. Sci.* **197-198**, 791-795.
29. Barrett, C. J., A. Natansohn and P. Rochon (1996) Mechanism of optically inscribed high-efficiency diffraction gratings in azo polymer. *J. Phys. Chem.* **100**, 8836-8842.

30. Watanabe, O., M. Tsuchimori, A. Okada and H. Ito (1997) Mode selective polymer channel waveguide defined by the photoinduced change in birefringence. *Appl. Phys. Lett.* **71**, 750-752.
31. Rochon, P., A. Natansohn, C. L. Callender and L. Robitaille (1997) Guided mode resonance filters using polymer films. *Appl. Phys. Lett.* **71**, 1008-1010.
32. Kawata, Y., Y. Aoshima, C. Egami, M. Ishikawa, O. Sugihara, O. Okamoto, M. Tsuchimori and O. Watanabe (1999) Light-induced surface modification of urethane-urea copolymer film used as write-once optical memory. *Jpn. J. Appl. Phys.* **38**, 1829-1831.
33. Egami, C., Y. Kawata, Y. Aoshima, S. Alasfar, O. Sugihara, H. Fujimura and N. Okamoto (2000) Two-stage optical data storage in azo polymers. *Jpn. J. Appl. Phys.* **39**, 1558-1561.
34. Naito, T., K. Horie and I. Mita (1991) The effect of polymer rigidity on photoisomerization of 4-dimethylamino-4'-nitroazobenzene. *Polym. Journal.* **23**, 809-813.
35. Saibi, R. L., K. Nakatani, J. A. Delaire, M. Dumont and Z. Sekkat (1993) Photoisomerization and second harmonic generation in disperse red one-doped and -functionalized poly(methyl methacrylate) films. *Chem. Mater.* **5**, 229-236.
36. Ronayette, J., R. Arnaud and J. Lemaire (1974) Isomérisation photosensibilisée par des colorants et photoréduction de l'azobenzène en solution. II. *Can. J. Chem.* **52**, 1858-1867.
37. Watanabe, O., M. Tsuchimori and A. Okada (1996) Two-step refractive index changes by photoisomerization and photobleaching processes in the films of non-linear optical polyurethanes and a urethane-urea copolymer. *J. Mater. Chem.* **6**, 1487-1492.
38. Allen, N. S. (1994) Photofading and light stability of dyed and pigmented polymers. *Polym. Deg. & Stab.* **44**, 357-374.
39. Nakanishi, M., O. Sugihara, N. Okamoto and K. Hirota (1998) Ultraviolet photobleaching process of azo dye doped polymer and silica films for fabrication of nonlinear optical waveguides. *Appl. Opt.* **37**, 1068-1073.
40. Albini, A., E. Fasai and S. Pietra (1982) The photochemistry of azo-dyes. The wavelength-dependent photoreduction of 4-diethylamino-4'-nitroazobenzene. *J. Chem. Soc. Perkin Trans.* 2, 1393-1395.
41. Vydra, J., H. Beisinghoff, H. Feix, M. Eckl, P. Strohriegl, W. Gortz and M. Eich (1996) Photobleaching mechanisms in azobenzene functionalized polymethacrylates. *Photoactive Org. Mater.* 401-410.
42. Gonzalez, A. G., M. Canva, G. I. Stegeman, R. Twieg, T. C. Kowalczyk and H. S. Lackritz (1999) Effect of temperature and atmospheric environment on the photodegradation of some disperse Red 1-type polymers. *Opt. Lett.* **24**, 1741-1743.